JOURNAL OF MATERIALS SCIENCE 32 (1997) 5215–5223

Nucleation and growth kinetics of reaction-product formation for copper–titanium and silver–titanium alloys on alumina

A. MEIER, PR. CHIDAMBARAM, G. R. EDWARDS, S. LIU
Center for Welding and Joining Research, Department of Metallurgical and Materials Engineering, Colorado School of Mines, Golden, CO 80401, USA

A nucleation and growth mechanism is proposed for the formation of the reaction product at the interface between polycrystalline alumina and liquid-metal alloy drops containing titanium. The reaction product had been previously identified to be an oxide of titanium. The growth of reaction product islands was clearly observed at the alumina–metal interface using optical microscopy after dissolving the metal droplets with acid. The fractional coverage was quantified as a function of time and, by assuming Avrami-type reaction kinetics, surface reaction rate constants, k, were calculated for copper–titanium and silver–titanium alloys on alumina. Reaction rate constants between 1.4×10^{-4} and $18 \times 10^{-4}\,s^{-2}$ were obtained for copper–titanium alloys on alumina. The k values for silver–titanium alloys were found to be an order of magnitude lower (2.5×10^{-6} and $7.2 \times 10^{-6}\,s^{-2}$) then the k values obtained for copper–titanium alloys on alumina.

1. Introduction

Applications for joining advanced ceramics to metals and dissimilar ceramics exist in the aerospace, automotive, nuclear and electronic industries [1–7]. A viable joining method is direct brazing, utilizing a ductile filler metal with an active metal addition. The active metal in the liquid promotes the wetting of the ceramic substrate through the formation of a reaction product at the ceramic–metal interface. Titanium is a popular active metal addition to a copper-based filler metal. When the titanium alloy is in contact with alumina, a titanium oxide reaction layer forms [8]. The control of this reaction is important because insufficient reaction leads to incomplete bonding, which results in joint degradation [9–11]. Excessive reaction and consequent reaction-layer thickening can also lead to a degradation of the joint mechanical properties [11, 12]. Thus, an understanding of the kinetics of the interfacial reactions is needed to obtain optimal joint properties.

When a liquid metal is in contact with alumina at high temperatures, the liquid spreads to form a wetting contact angle. The premise of the mechanism proposed in this work is that the final contact angle is a result of the decrease in interfacial energy caused by reaction-layer formation. The progressive decrease in the contact angle observed as a function of time is related to the rate of coverage of the surface by the reaction product beneath the liquid drop. In this paper, an attempt is made to quantify the reaction layer formation (surface coverage) rates.

While the reaction-product thickening kinetics have been quantitatively described for reactive metal/ceramic systems [8, 14–17], the surface-coverage rate has not been quantitatively analysed. The thickening rates are frequently rapid [18] and a complete interfacial reaction-product layer is assumed at all times. For a reactive metal droplet on a ceramic substrate, the reaction-product formation mechanism is not clearly understood. Most existing theories predict complete reaction-layer formation at the interface [8, 19, 20].

According to the existing models, the drop spreads beyond the ceramic/metal/vapour triple point by reaction on the ceramic substrate ahead of the triple point. The reactive metal moves to the unreacted ceramic surface by either a surface diffusion or evaporation/condensation process [21, 22] and the spreading rate is determined by the rate at which reactive metal moves ahead of the triple point.

In this study, different reaction-product formation and spreading mechanisms are proposed. Instead of reaction-product formation ahead of the triple point and, consequently, a complete reaction-product layer at the ceramic/metal interface, an Avrami-type surface nucleation and growth kinetics mechanism is suggested. In this mechanism, islands of reaction-product nucleate and grow at the ceramic/metal interface until a complete interfacial layer eventually forms. The drops then spread because, as the fractional coverage of the surface increases, the energy of the ceramic/metal interface decreases and the spreading force increases. The mechanism of drop spreading is discussed in greater detail elsewhere [23].

0022–2461

2. Experimental procedure

A method was developed for measuring the fractional coverage of an alumina/liquid metal interfacial reaction product as a function of time. Two systems were chosen for this investigation: copper–titanium/alumina and silver–titanium/alumina. The metal systems chosen were both simple binary systems with a non-reactive base metal (copper or silver) and a reactive metal addition (titanium). Binary systems were studied instead of the ternary and quaternary systems used in commercial brazing, so that complications due to the interactions between the different components could be avoided. First, the copper–titanium system was chosen because many of the currently used brazing alloys contain these two materials and because the furnace used was limited to approximately 1500 °C, precluding the use of pure titanium. Several copper–titanium intermetallics exist for this system; however, above 1000 °C, only a single liquid-phase exists for approximately 45–95 wt% titanium (Fig. 1). The silver–titanium system was chosen for comparison with the copper–titanium system. Only low-titanium compositions can be studied for this system owing to a large solid–liquid two-phase field (Fig. 2).

The substrates used for all of the tests were 0.64 mm thick Coors AD-996 polycrystalline alumina substrates. The Coors AD-996 electronic substrate has a surface roughness of 75–125 μm (CLA), an average grain size of approximately 1.2 μm, and an impurity concentration of 0.4% [24]. The substrates were cleaned with nitric acid and rinsed with ethanol before testing. Copper (99.99% purity), silver (99.9% purity) and titanium (99.99% purity) blocks were used as the starting materials for the metal alloys.

A tube furnace with a viewing window was used to obtain *in situ* diameter measurements of the spreading of the liquid metal drops. The furnace configuration has been discussed in greater detail elsewhere [23, 25, 26]. The system recirculated argon through an oxygen scavenger to reduce the oxygen partial pressure to approximately 0.006 pa (50 p.p.b). The tests were performed at an argon overpressure of approximately 10 kPa. The nitrogen partial pressure, determined from the known purity of the argon, was estimated to be 1 Pa (10 p.p.m.). The spreading of the drops was videotaped and the spreading diameter was measured from the videotape by freezing frames on a Leco image analyser.

The fractional coverage of the alumina surface by the reaction product was determined as a function of time using short-duration sessile drop tests. A sample configuration was employed which ensured a minimum of non-isothermal exposure time [26]. In this configuration, liquid copper was brought into contact with solid titanium already at the desired test temperature. For all of the tests, a 2.0 g liquid metal drop was allowed to spread on an alumina substrate for between 20 and 600 s under an argon atmosphere. The furnace was then shut down and the sample was exposed to air, which oxidized the titanium and stopped spreading. After cooling to room temperature, the metal drops were dissolved by successively placing the samples in concentrated nitric and hydrochloric acids. The acid dissolves the metals relatively rapidly and leaves behind the oxide-based reaction product [8]. This fact was also verified in this study by treating the sample in acid for extended periods. The reaction product was stable even after acid treatment for 1 d. The ceramic surfaces were then magnified 200 to 1000

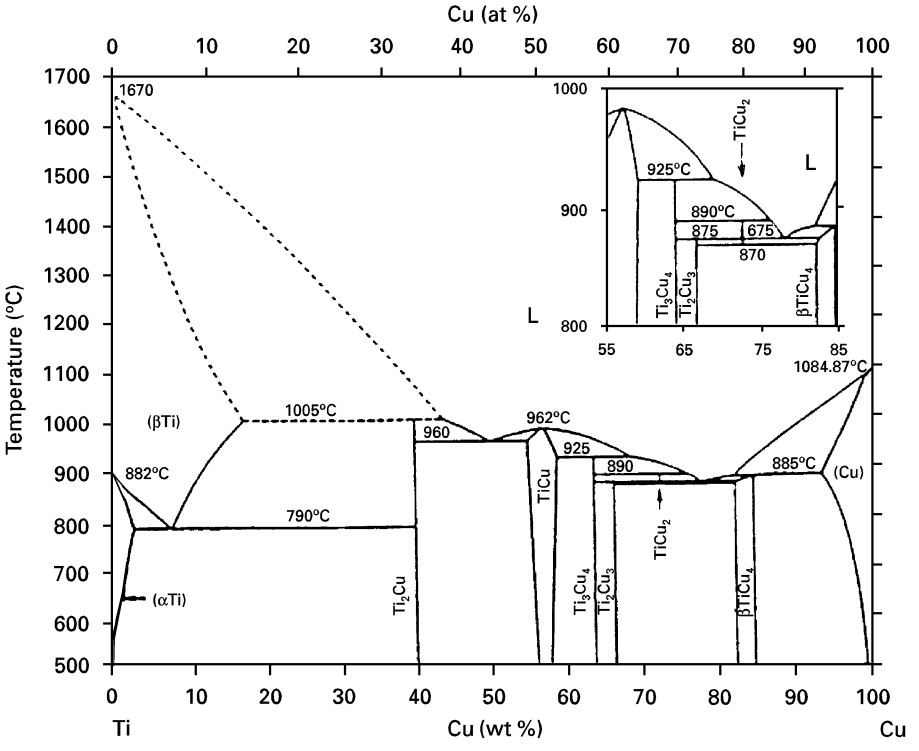

Figure 1 Copper–titanium phase diagram [36].

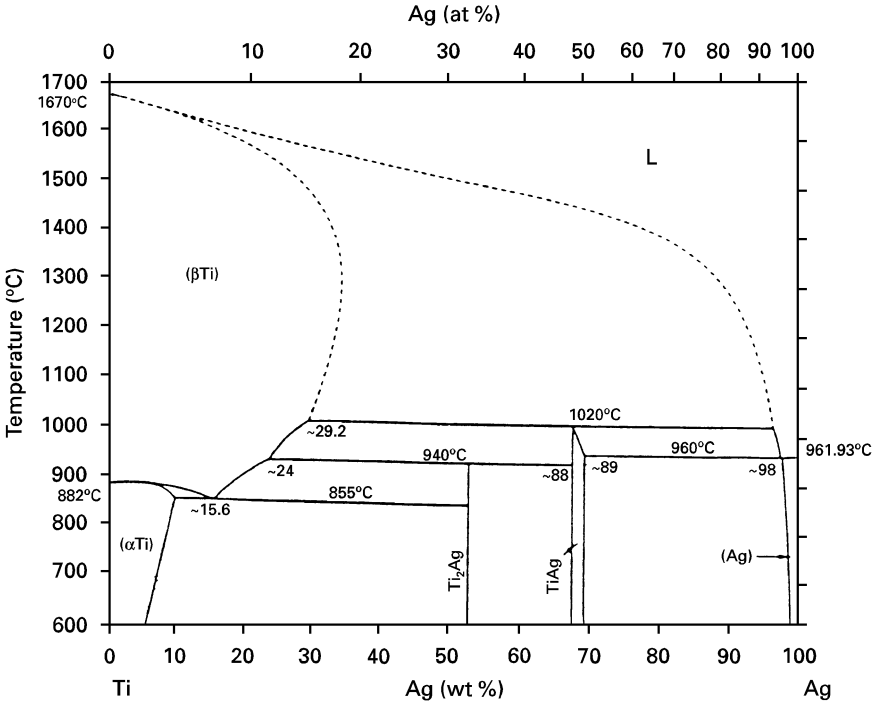

Figure 2 Silver–titanium phase diagram [36].

times under a light microscope and the images were transferred to a Leco image analyser, where the fractional coverages were determined using the Leco 2001 software package. Varying coverage fractions (each representing a different annular region) were correlated with their respective coverage times based on analyses of the videotapes of the spreading. Relatively large drops (2.0 g) were used to maximize the interfacial area. Three sessile drop tests of varying times were performed for each composition and temperature to minimize surface roughness and surface cleanliness effects.

In the copper–titanium/alumina system, large spreading radius changes occurred even for very short times (less than 100 s). Upon dissolution of the metal, concentric rings of reaction product of varying fractional coverage of the original alumina surface were observed on these samples. The reaction product has been identified to be an oxide of titanium [8]. Fig. 3 shows both the observed microstructure and the schematic diagram. Thus, 5–11 coverage fractions were quantified for the three samples at each test condition. Ten area fraction measurements were made on each visibly different coverage region, and the average fractional coverage and the standard deviation of the mean were determined. The reaction times for each coverage region were determined by matching the diameter versus time data to the different reaction-product rings on the substrate. Fractional coverage measurements were made for times ranging from 30–390 s.

Only three fractional coverage measurements were obtained for the silver–titanium/alumina test condition because the relatively small radius changes limited the fractional coverage measurements to the initially covered region for each sample. Outside of the initially covered region, it was difficult to match the fractional coverage rings with time. For this system, 15 area fraction measurements were made in each coverage region and then averaged. The tests lasted for 40–600 s.

For the copper–titanium/alumina system, temperatures varied from 1120–1200 °C and titanium concentrations varied from 3–20 wt%. For the silver–titanium/alumina system, temperatures of 1000 and 1100 °C, and titanium compositions from 1–5 wt% were studied. The test matrix for the copper–titanium/alumina system is presented in Table I and the test matrix for the silver–titanium/alumina system is presented in Table II.

3. Results

3.1. Copper–titanium/alumina system

First, utilizing the improved sessile drop technique [26], an experiment was performed for verification of product nucleation and growth at the ceramic–metal interface. Molten copper was dropped on to solid titanium which was resting on alumina at approximately 1200 °C. After dissolving the titanium, the liquid metal alloy was allowed to spread for approximately 120 s. After cooling, the metal was dissolved using nitric and hydrochloric acids and the alumina surface was examined using optical microscopy.

The microstructure at several metal/ceramic contact radii is shown in Fig. 3. The initially covered surface is completely covered with reaction product. Outside of the initial radius, islands of reaction product are observed. The fraction of the surface covered with reaction product decreases as the relative coverage time decreases (as the radial distance increases). Finally, no reaction product was observed outside of the liquid metal/substrate contact area. The presence of reaction-product islands beneath the drop supports

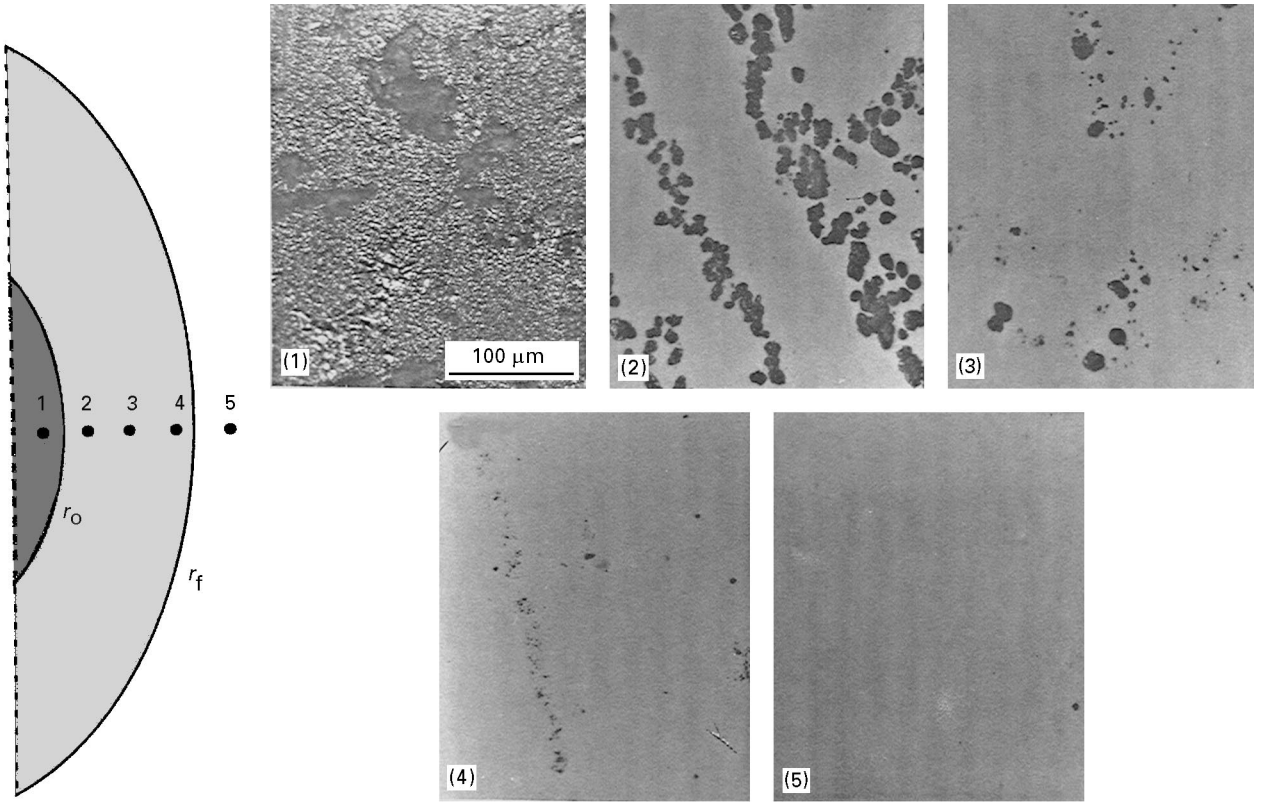

Figure 3 Microstructure of the alumina surface after dissolution of the copper–titanium drop. The initially covered area, $r > r_0$, is completely covered with reaction product (1). Reaction-product islands are observed in the spreading region, $r_0 < r < r_f$, (2–4). No reaction product is observed outside of the spreading area, $r > r_f$ (5).

TABLE I Copper–titanium/alumina test matrix

Ti (wt %)	Temperature (°C)		
	1120	1160	1200
3	X		
5	X	X	X
7	X		
10	X	X	X
20	X	X	X

TABLE II Silver–titanium/alumina test matrix

Ti (wt %)	Temperature (°C)	
	1000	1100
1		X
3		X
5	X	X

reaction-product nucleation and growth. The absence of reaction product ahead of the drop liquid/vapour/substrate triple point suggests that a metal volatilization and condensation mechanism does not promote spreading in this system.

While the type of reaction product formed is important in determining both the relative wettability and the mechanical properties of a ceramic/metal joint, the compositional characterization of the reaction products can be complicated and was beyond the scope of this study. Several authors have studied the reaction products formed between titanium/alumina and copper–titanium/alumina couples using both experimental and theoretical thermodynamic approaches [13, 14, 27–32]. The reaction-layer sequences identified were different for each study and appeared to be dependent upon both the test conditions and the analytical techniques utilized.

The fractional coverage of an alumina substrate by reaction product for copper–titanium alloys is shown as a function of time in Figs 4–14. The error bars represent the standard deviation of the mean for ten measurements performed for each sample condition. The three different symbols on each plot represent results from three different sample runs. While significant variance in the data is evident, the increase in fractional coverage with time is still apparent. Several of the plots show a clear increase in fractional coverage with time. For example, 10 wt% titanium at 1160 °C (Fig. 10), 20 wt% titanium at 1160 °C (Fig. 11), and 10 wt% titanium at 1200 °C (Fig. 13) all exhibit a continuous increase in coverage with increasing time. Other test conditions displayed an increase in coverage with time for a given sample but with a poor correlation between different samples. Samples exhibiting this type of behaviour are 5 wt% titanium at 1120 °C (Fig. 5), 7 wt% titanium at 1120 °C (Fig. 6), 10 wt% titanium at 1120 °C (Fig. 7), 20 wt% titanium at 1120 °C (Fig. 8), 5 wt% titanium at 1160 °C (Fig. 9), 5 wt% titanium at 1200 °C (Fig. 12) and 20 wt% titanium at 1200 °C

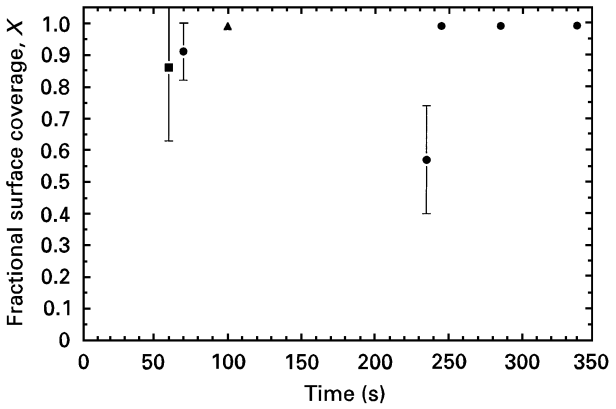

Figure 4 Fractional coverage of reaction product on the alumina surface as a function of time for a copper–3 wt % titanium alloy at 1120 °C. The three different symbols represent three independent sample runs. The error bars are the standard deviation of the mean for ten measurements.

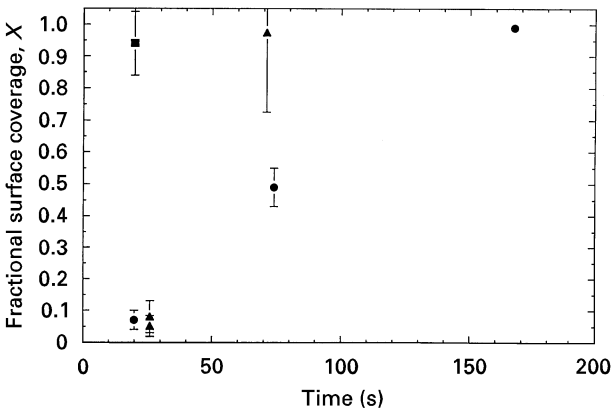

Figure 5 Fractional coverage of reaction product on the alumina surface as a function of time for a copper–5 wt % titanium alloy at 1120 °C. The three different symbols represent three independent sample runs. The error bars are the standard deviation of the mean for ten measurements.

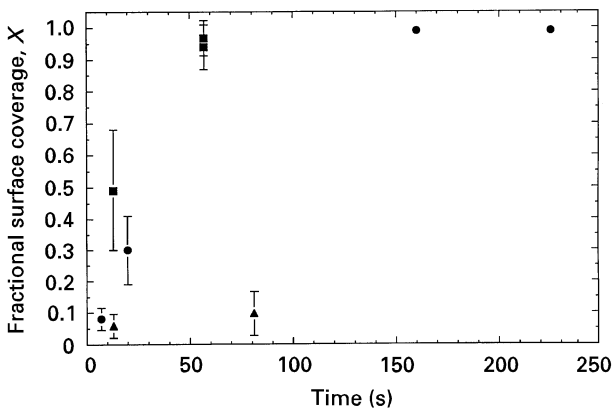

Figure 6 Fractional coverage of reaction product on the alumina surface as a function of time for a copper–7 wt % titanium alloy at 1120 °C. The three different symbols represent three independent sample runs. The error bars are the standard deviation of the mean for ten measurements.

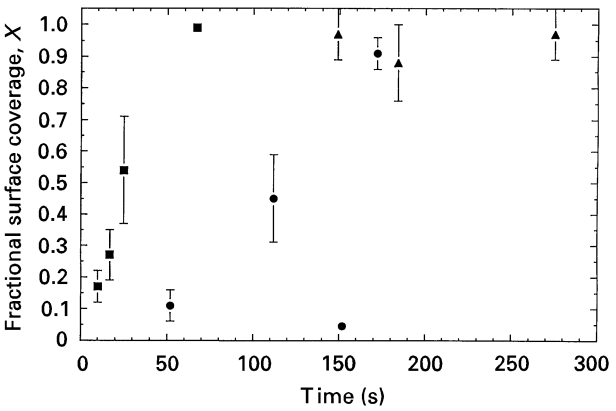

Figure 7 Fractional coverage of reaction product on the alumina surface as a function of time for a copper–10 wt % titanium alloy at 1120 °C. The three different symbols represent three independent sample runs. The error bars are the standard deviation of the mean for ten measurements.

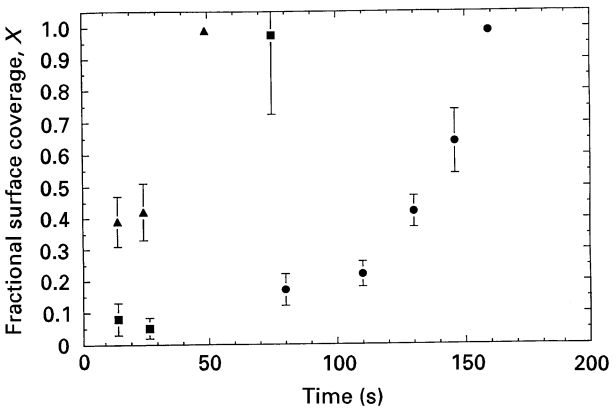

Figure 8 Fractional coverage of reaction product on the alumina surface as a function of time for a copper–20 wt % titanium alloy at 1120 °C. The three different symbols represent three independent sample runs. The error bars are the standard deviation of the mean for ten measurements.

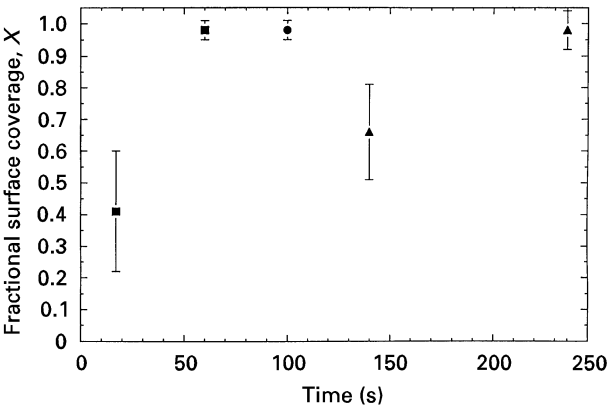

Figure 9 Fractional coverage of reaction product on the alumina surface as a function of time for a copper–5 wt % titanium alloy at 1160 °C. The three different symbols represent three independent sample runs. The error bars are the standard deviation of the mean for ten measurements.

(Fig. 14). A significant decrease in coverage with time was only observed for a single test condition (3 wt % titanium samples at 1120 °C), and this was only a single data point (Fig. 4).

Representative fractional coverage micrographs are shown in Fig. 15. Initially, the reaction product forms small islands (Fig. 15a). The islands grow together (Fig. 15b) until islands of non-reacted alumina are

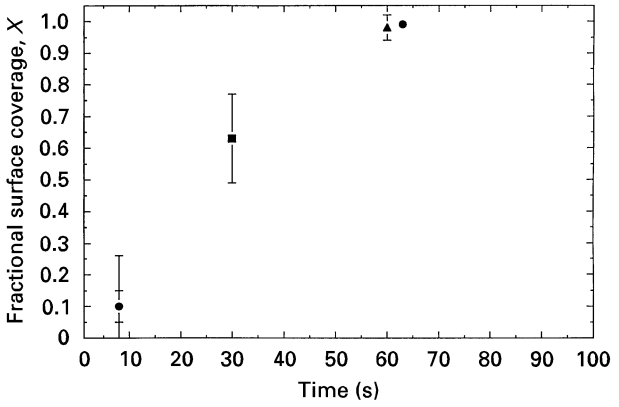

Figure 10 Fractional coverage of reaction product on the alumina surface as a function of time for a copper–10 wt % titanium alloy at 1160 °C. The three different symbols represent three independent sample runs. The error bars are the standard deviation of the mean for ten measurements.

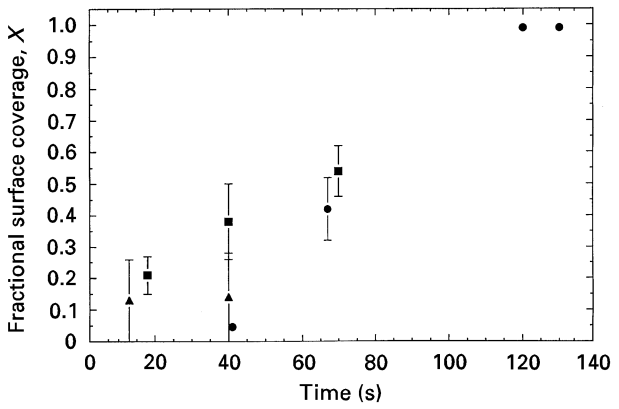

Figure 11 Fractional coverage of reaction product on the alumina surface as a function of time for a copper–20 wt % titanium alloy at 1160 °C. The three different symbols represent three independent sample runs. The error bars are the standard deviation of the mean for ten measurements.

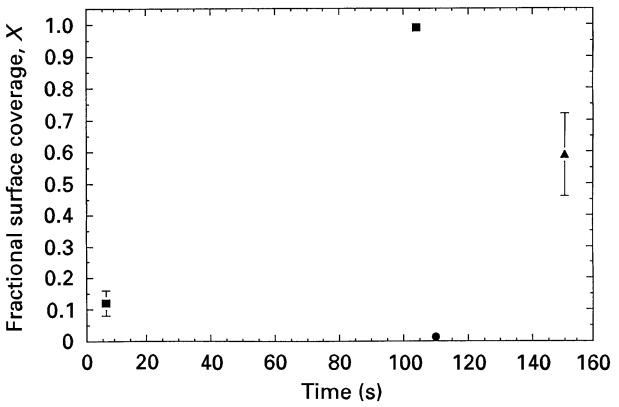

Figure 12 Fractional coverage of reaction product on alumina surface as a function of time for a copper–5 wt % titanium alloy at 1200 °C. The three different symbols represent three independent sample runs. The error bars are the standard deviation of the mean for ten measurements.

surrounded by reaction product (Fig. 15c). Finally, the entire surface is covered by reaction product (Fig. 15d). The large standard deviation of some fractional coverage measurements was partially caused by

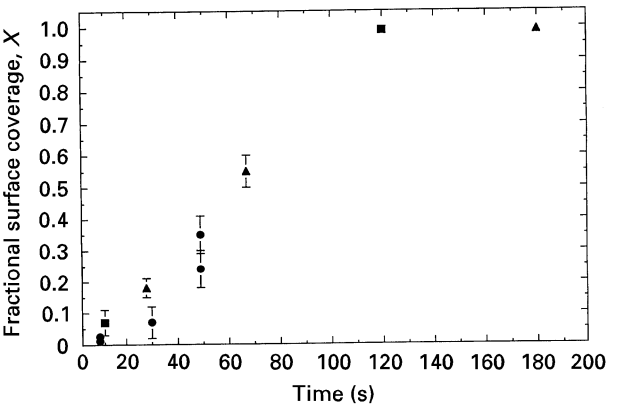

Figure 13 Fractional coverage of reaction product on the alumina surface as a function of time for a copper–10 wt % titanium alloy at 1200 °C. The three different symbols represent three independent sample runs. The error bars are the standard deviation of the mean for ten measurements.

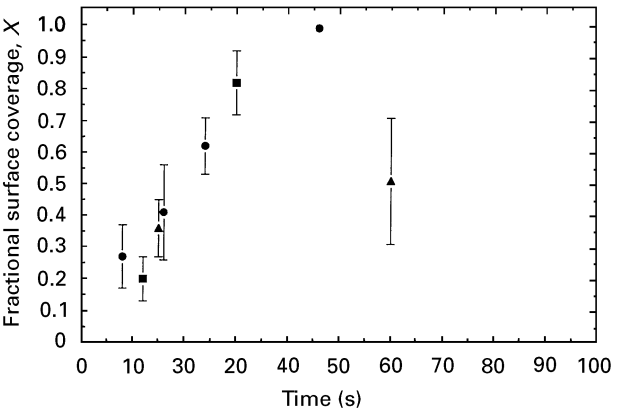

Figure 14 Fractional coverage of reaction product on the alumina surface as a function of time for a copper–20 wt % titanium alloy at 1200 °C. The three different symbols represent three independent sample runs. The error bars are the standard deviation of the mean for ten measurements.

non-uniform growth of the islands. The very large reaction-product islands or alumina islands shown in Fig. 15b and c were randomly dispersed in a given coverage region.

3.2. Silver–titanium/alumina system

The fractional coverage observed for silver–titanium alloys on alumina is plotted versus time in Fig. 16. The error bars represent the standard deviation of the mean for 15 measurements at each test condition. All four test conditions exhibited similar coverage behaviour. The fractional coverage was very small (less than 5%) for the first 300 s. The coverage then increased with increasing time. The silver–titanium/alumina system behaved similar to the copper–titanium/alumina system except that the coverage rate was much slower for the silver–titanium/alumina system. While greater than 99% coverage was frequently obtained in less than 100 s for copper–titanium alloys on alumina, complete reaction product coverage was not obtained for silver–titanium alloys on alumina after 600 s.

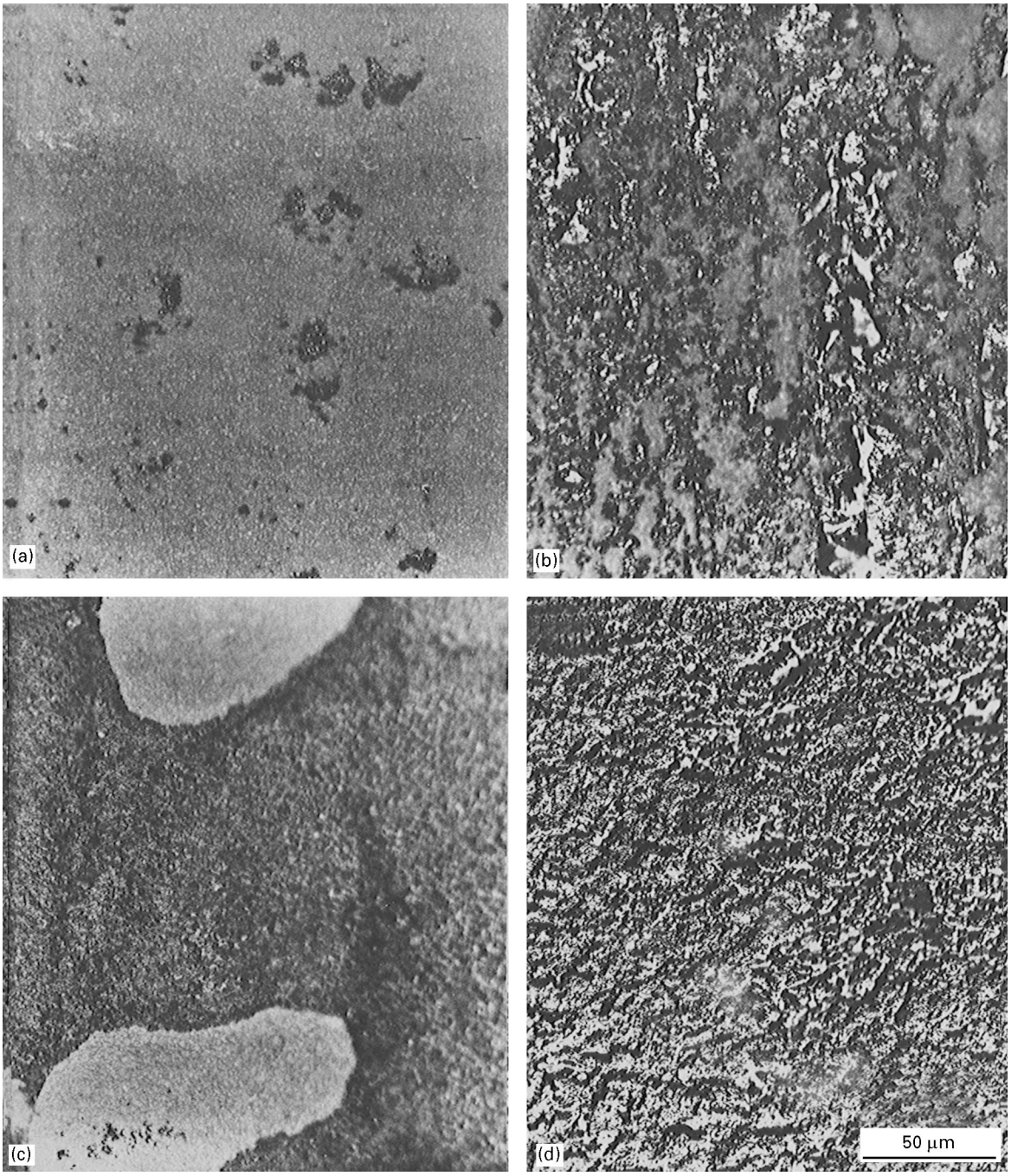

Figure 15 Micrographs of fractional coverage of reaction product on the alumina surfaces for copper–titanium alloys: (a) initial islands form, (b) islands grow together, (c) alumina islands are left, and (d) complete coverage is obtained

Representative fractional coverage micrographs are shown in Fig. 17. The island formation was similar to the island formation observed for copper–titanium alloys on alumina except that a more needle-like product growth was observed for the silver–titanium alloys on alumina.

4. Discussion

4.1. Calculation of surface reaction rate constant

The surface reaction rate constant, k, can be determined from fractional coverage rates measured as a function of composition and temperature. It should be stressed that this is the rate constant for the formation of a monolayer of reaction product on the surface of the ceramic substrate, which is not the same as the rate constant for parabolic thickening. In general, the monolayer formation rate constant should be greater than the parabolic rate constant, because the surface layer must form before the reaction product can significantly thicken. The reaction rate constants would only be similar if the surface nucleation rate was very slow and the bulk diffusion rates of the reacting species were very high, so that only a few islands of reaction product would nucleate and grow into the substrate. The completion of the surface monolayer would then occur by the coalescence of the large

product "islands", and the growth rate would be approximately the same in all directions.

While the values for the parabolic thickening rate have been reported for several systems [13–16], the rate of surface coverage has not been quantitatively studied. This is because the commercially successful alloys have very rapid coverage rates, achieving total coverage in only a few seconds.

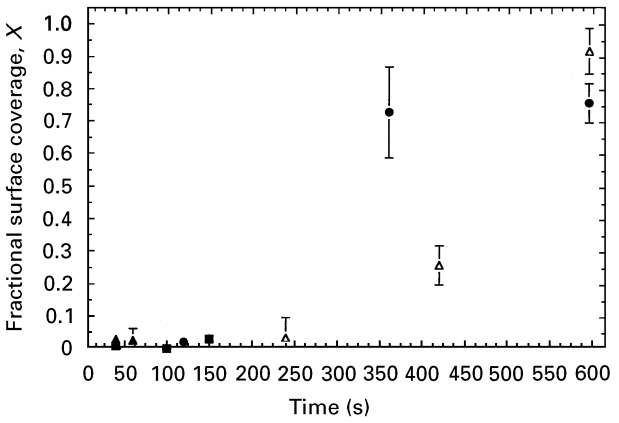

Figure 16 Fractional coverage of reaction product on the alumina surface as a function of time for silver–titanium alloys at (△) 1000 and (●, ■, ▲) 1100 °C. The error bars are the standard deviation of the mean for 15 measurements. (△, ▲) Ag-5 wt%, Ti, (●) Ag-1 wt% Ti, (■) Ag-3 wt% Ti.

The fractional coverage rate for two-dimensional surface nucleation and growth is given by the Avarami equation [33–35]

$$X = 1 - \exp(-kt^2) \quad (1)$$

If the fractional coverage is known for a given time, the reaction rate constant, k, can be calculated. At each composition and temperature, the mean value of k and the standard deviation of the mean were calculated, and are shown in Table III. The k values ranged from 0.144×10^{-3} to $1.849 \times 10^{-3}\,s^{-2}$. The standard deviation of the mean was very large. In one case (5 wt% Ti at 1200 °C) it was larger than k itself.

For the silver–titanium/alumina system, the k values ranged from 2.56×10^{-6} to $7.29 \times 10^{-6}\,s^{-2}$, values an order of magnitude smaller than the copper–titanium/alumina k values. The average k values and the standard deviation of the mean are given in Table IV.

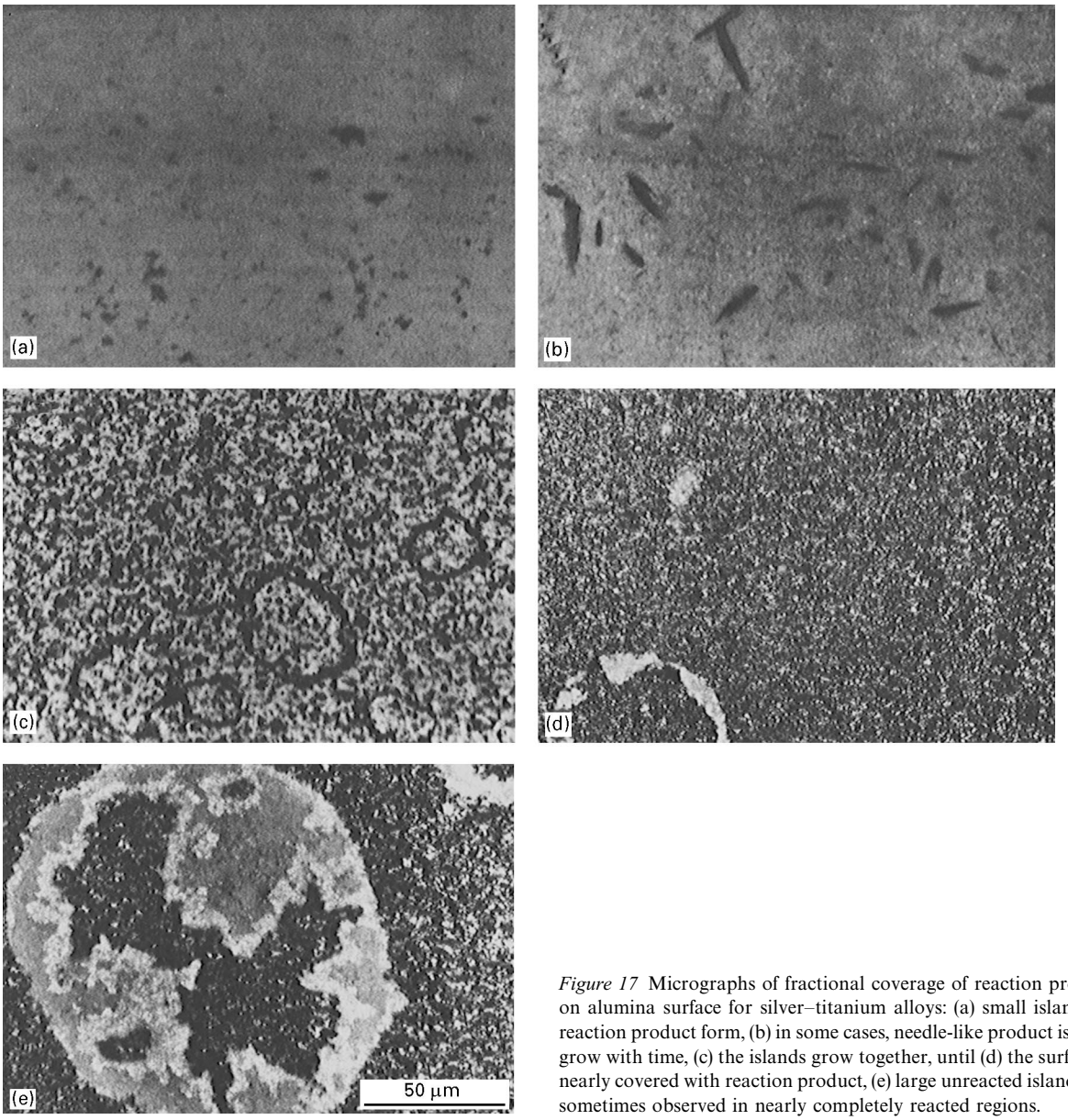

Figure 17 Micrographs of fractional coverage of reaction product on alumina surface for silver–titanium alloys: (a) small islands of reaction product form, (b) in some cases, needle-like product islands grow with time, (c) the islands grow together, until (d) the surface is nearly covered with reaction product, (e) large unreacted islands are sometimes observed in nearly completely reacted regions.

TABLE III The average surface reaction rate constant, k, for copper–titanium alloys on polycrystalline alumina. The uncertainties are the standard deviation of the mean

T (°C)	Ti (wt %)	k (10^{-6} s^{-2})
1120	3	144 ± 49
1120	5	196 ± 36
1120	7	841 ± 256
1120	10	289 ± 256
1120	20	529 ± 289
1160	5	484 ± 256
1160	10	1296 ± 16
1160	20	400 ± 169
1200	5	484 ± 729
1200	10	256 ± 25
1200	20	1849 ± 225

TABLE IV The average surface reaction rate constant, k, for silver–titanium alloys on polycrystalline alumina. The uncertainties are the standard deviation of the mean

T (°C)	Ti (wt %)	k (10^{-6} s^{-2})
1000	5	2.56 ± 1
1100	1	4.41 ± 1
1100	3	1.44 ± 1.21
1100	5	7.29 ± 2.25

5. Conclusion

The proposed reaction-product island nucleation and growth mechanism is qualitatively correct based on micrographs and measurements of the increase in fractional coverage of the ceramic/metal interface by reaction product with increasing time. The photo-micrographs refute the currently accepted mechanisms which assume a complete reaction-product layer formation ahead of the solid/liquid/vapour triple point.

Reaction rate constants of between 1.4×10^{-4} and 18×10^{-4} s^{-2} were obtained for copper–titanium alloys on alumina. The k values for silver–titanium alloys were determined to be between 2.5×10^{-6} and 7.2×10^{-6} s^{-2}, values which are an order of magnitude lower than the k values obtained for copper–titanium alloys on alumina.

Acknowledgements

This research was funded by the Office of Naval Research, Contract N0014-91-J-4049. The Support of Dr George Yoder, ONR, is gratefully acknowledged. We would also like to acknowledge the Leco Corporation (through Mr Dwight Warren and Mr Dennis Coons) and the AMAX Foundation (through Dr Chet Van Tyne) for the loan of the videotaping equipment and to thank Mr Scott Pawelka, CSM, for his technical assistance with the experimental aspects of this work.

References

1. R. LOEHMAN, *Ceram. Bull.* **68**(4) (1989) 891.
2. M. G. NICHOLAS and R. J. LEE, *Metals Mater.* **5** (1989) 348.
3. P. POPPER, in "Energy and Ceramics, Proceedings of the 4th International Meeting on Modern Ceramics Technologies", edited by P. Vincenzini (Elsevier Scientific, Amsterdam, 1980) 569.
4. H. MIZUHARA, *Adv. Mater. Proc. Metal Progress* **2**(87) (1987) 53
5. R. R. KAPOOR and T. W. EAGAR, *J. Am. Ceram. Soc.* **72** (1989) 448.
6. A. J. MOOREHEAD and H. KEATING, *Weld. J.* **65**(10) (1986) 17.
7. S. MUSIKANT, "What Every Engineer Should Know About Ceramics" (Marcel Dekker, New York, 1991) Chs 7, 12 and 13.
8. P. R. CHIDAMBARAM, G. R. EDWARDS and D. L. OLSON, *Metall. Mater. Trans.* **25A** (1994) 2083.
9. M. MORITA, K. SUGANUMA and T. OKAMOTO, *J. Mater. Lett.* **6** (1987) 474.
10. M. Y. HE and H. G. EVANS, *Acta Metall.* **39** (1991) 1587.
11. V. TVERGAARD, *ibid.* **39** (1991) 419.
12. G. ELSSNER and G. PETZOW, *ISIJ Int.* **30** (1990) 1011.
13. K. SUGANUMA, T. OKAMOTO, M. KOIZUMI and M. SHIMADA, *J. Mater. Sci.* **22** (1987) 1359.
14. T. OKAMOTA, *ISIJ Int.* **30** (1990) 1033.
15. R. E. TRESSLER, T. L. MOORE and R. L. CRANE, *J. Mater. Sci.* **8** (1973) 151.
16. D. H. KIM, S. H. HWANG and S. S. CHUN, *ibid.* **26** (1991) 3223.
17. W. J. WHATLEY and F. E. WAWNER, *J. Mater. Sci. Lett.* **4** (1985) 173.
18. T. KUZUMAKI, T. ARIGA and Y. MIYAMOTA, *ISIS Int.* **30** (1990) 1135.
19. V. LAURENT, D. CHATAIN and N. EUSTATHOPOULOS, *Mater. Sci. Eng.* **A135** (1991) 89.
20. P. KRISTALIS, L. COURDIER and N. EUSTATHOPOULOS, *J. Mater. Sci.* **26** (1991) 3400.
21. G. C. SMITH and C. LEA, *Surf. Interface Anal.* **9** (1960) 145.
22. P. C. WAYNER and J. SCHONBERG, *J. Coll. Int. Sci.* **152** (1992) 507.
23. A. MEIER, PhD thesis, Colorado School of Mines Thesis no. T-4667 (1994).
24. "Thin Film Substrate Technical Specifications 10-2-0692", Coors Ceramics Company-Electronics, Golden, CO 80401, USA 1992.
25. A. MEIER, P. R. CHIDAMBARAM, V. GABRIEL and G. R. EDWARDS, in "Processing and Fabrication of Advanced Materials III", edited by V. A. Ravi, T. S. Srivatsan and J. J. Moore, ASM International, Materials Park, OH. ASM/TMS Proceedings, 1994, pp. 47–58.
26. A. MEIER, P. R. CHIDAMBARAM and G. R. EDWARDS, *J. Mater. Sci.* **30** (1995) 3791.
27. F. S. OHUCHI and M. KOHYAMA, *J. Am. Ceram. Soc.* **74** (1991) 1163.
28. R. E. LEOHMAN and A. P. TOMSIA, *Acta Metall. Mater.* **40** suppl. (1992) 575.
29. X. L. LI, R. HILLEL, F. TEYSSANDIER, S. K. CHOI and F. J. J. VAN LOO, *ibid.* **40** (1992) 3149.
30. F. HATAKEYAMA, K. SUGANUMA and T. OKAMOTO, *J. Mater. Sci.* **21** (1986) 2455.
31. M. NAKA, K. ASAMI, I. OKAMOTO and Y. ARATA, *Trans. JWRI* **12** (1983) 145.
32. K. S. BANG and S. LIU, *Weld. J.* **73**(3) (1994) 54s.
33. M. AVRAMI, *J. Phys. Chem.* **7** (1939) 1103. "II", *ibid.*, **8**(2), (1940), p. 212; "III" *ibid.*, **9**(2), (1941).
34. *Idem*, *ibid.* **8** (1940) 212.
35. *Idem*, *ibid.* **9** (1941) 177.
36. T. B. MASSLASKI (Ed.), "Binary Alloy Phase Diagrams", Vols 1 and 2 (ASM International. Materials Park, OH, 1990) p. 106, 1495.

Received 15 December 1995
and accepted 10 February 1997